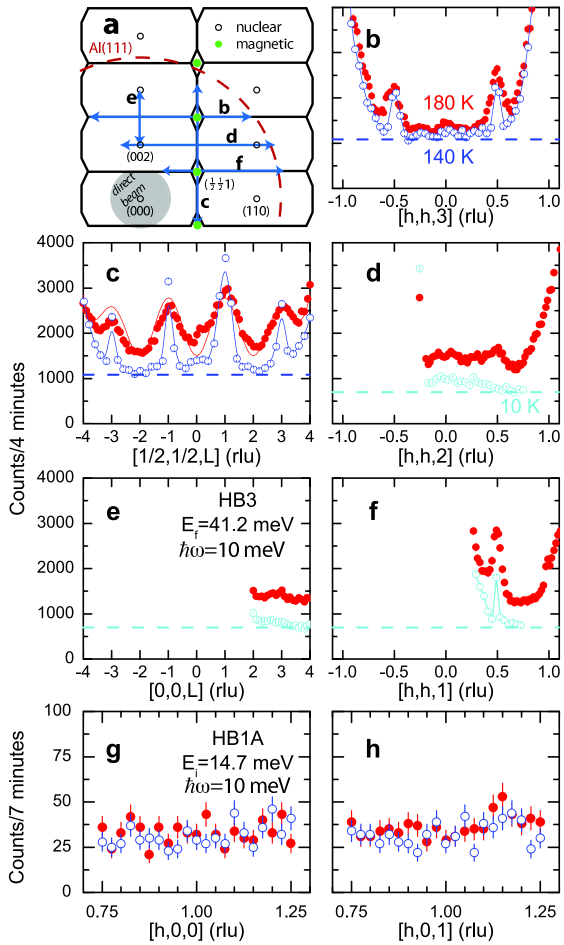

FIG. 1: Summary of scans performed at $T = 10$ K, 140 K (empty symbols) and 180 K (filled symbols) on HB3 ($E_f = 41.2$ meV) and HB-1A with spectrometer configurations described in the text. (a) shows (hhL) plane in reciprocal space where the scans at HB3 were performed. (b)-(f) shows the various cuts investigated, as indicated in (a). (g) and (h) show the scans performed in the ($h0L$) plane using HB1A. No diffuse magnetic scattering was observed in the ($h0L$) plane. The magnetic signal is only observed centered at wavevectors $\mathbf{Q} = \mathbf{Q}_{\rm AFM}$.

tered intensity are also observed along the c-axis indicating a two-dimensional character to the paramagnetic fluctuations. In general, spin correlations weaken and broaden further in momentum and energy with increasing temperature, but are still observed up to the highest measured temperature of 300 K. These observations can be explained in the context of spin dynamics overdamped by particle-hole excitations. In particular, we use a phenomenological theoretical model with in-plane and interplane magnetic anisotropy to consistently fit our data for all temperatures, obtaining the ratios $J_1/J_2 \simeq 0.55$ and $J_c/J_2 \simeq 0.1$. We find that the spin fluctuations in the paramagnetic phase of the parent compound bear a close resemblance to the paramagnetic fluctuations in the superconducting compositions.

This article is laid out as follows. In section II below, the experimental conditions under which the experiment were performed and the sample details are presented. The data analysis and results are presented in section III. Finally, a discussion and a summary are given in section IV.

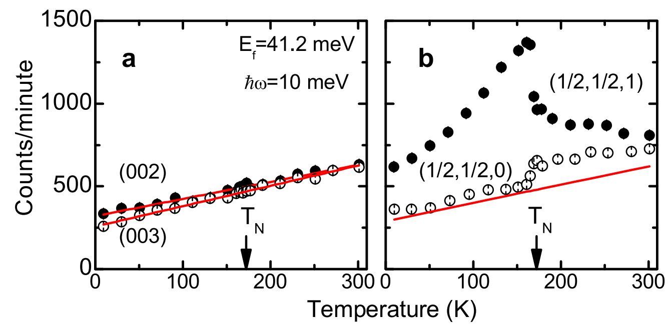

FIG. 2: Temperature evolution of the neutron scattering signal measured on HB3 at $\hbar\omega = 10$ meV. (a) Background estimate measured away from $\mathbf{Q}_{\rm AFM}$ at (002) (solid symbols) and (003) (open symbols) showing no anomaly at T_N. Solid lines are linear fits to the temperature dependent intensity. (b) Intensity at $\mathbf{Q}_{\rm AFM} = (1/2,\ 1/2,\ 1)$ and $(1/2,\ 1/2,\ 0)$. The solid line is the non-magnetic background estimate obtained from averaging the fits at (002) and (003), shown in panel (a).

II. EXPERIMENTAL PROCEDURES

Inelastic neutron scattering measurements were performed on a single crystal mosaic (∼400 small single-crystal samples) of $CaFe_2As_2$ with a total mass of ∼ 2 grams that are co-aligned to within 1.5 degrees full-width-at-half-maximum (FWHM). The preparation methods of the single-crystals have been described elsewhere.[24] Data were collected using the HB3 and HB1A triple-axis spectrometers at the High Flux Isotope Reactor at Oak Ridge National Laboratory and the MAPS chopper spectrometer at the ISIS facility at Rutherford Appleton Laboratory. HB3 was operated in relaxed resolution for measurement of the diffuse scattering signals in the paramagnetic phase, with fixed final energy (E_f) configurations, $E_f = 14.7$ meV and 41.2 meV, and 48’-60’-80’-120’ collimation. The sample was mounted in a closed-cycle refrigerator and oriented for scattering in the tetragonal (hhL) plane. HB1A was operated with fixed incident neutron energy of 14.7 meV and 48’-40’-40’-136’ collimation and the sample mounted in the ($h0L$) plane. The MAPS experiment was performed at T =180 K, with an incident energy of 100 meV using the same sample aligned with the c-axis along the incident beam direction.

To avoid confusion, the data is exclusively presented in tetragonal units and we define $\mathbf{Q} = \frac{2\pi}{a}(h\mathbf{i} + k\mathbf{j}) + \frac{2\pi}{c}L\mathbf{k}$ as the momentum transfer indexed according to the $I4/mmm$ tetragonal cell with lattice parameters $a = 3.88$ Å and $c = 11.74$ Å at 300 K. The vectors $\mathbf{i}$, $\mathbf{j}$ and $\mathbf{k}$ are the fundamental translation unit vectors in real space. For comparison with the AFM low temperature orthorhom-